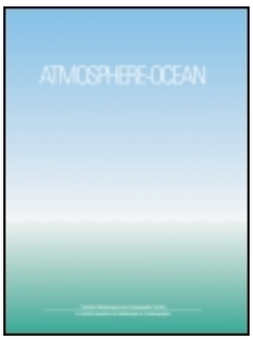

Atmosphere-Ocean

ISSN: 0705-5900 (Print) 1480-9214 (Online) Journal homepage: http://www.tandfonline.com/loi/tato20

Applications of the cyclic spectral analysis to the surface temperature fluctuations in a stochastic climate model and a GCM simulation

Jian-Ping Huang , Han-Ru Cho & >Gerald R. North

To cite this article: Jian-Ping Huang , Han-Ru Cho & >Gerald R. North (1996) Applications of the cyclic spectral analysis to the surface temperature fluctuations in a stochastic climate model and a GCM simulation, Atmosphere-Ocean, 34:4, 627-646, DOI: 10.1080/07055900.1996.9649580

To link to this article: http://dx.doi.org/10.1080/07055900.1996.9649580

Applications of the Cyclic Spectral Analysis to the Surface Temperature Fluctuations in a Stochastic Climate Model and a GCM Simulation

Jian-Ping Huang and Han-Ru Cho
Department of Physics
University of Toronto
Toronto, Ontario, Canada M5S 1A7

and

Gerald R. North
Climate System Research Program
Department of Meteorology
Texas A&M University, College Station, TX 77843-3150

[Original manuscript received 5 November 1995; in revised form 17 April 1996]

ABSTRACT *In this paper, we introduce the cyclostationary processes into climate analysis and undertake a systematic study of the cyclic spectra of surface temperature fluctuations. The technique is adapted from cyclostationarity theory in signal processing. To demonstrate the usefulness of this technique, a very simple cyclostationary stochastic climate model is constructed. Our results show that the seasonal cycle strongly modulates the amplitudes of the covariance and the spectrum. The technique was also applied to the surface temperature fluctuations in a fifteen-year seasonal run of the National Center for Atmospheric Research (NCAR) Community Climate Model (CCM2, R15) using a zonally symmetric all-land surface as the lower boundary. The results indicate that intraseasonal oscillations localized according to time of year are still present even after the surface temperature fields have been normalized using the commonly used procedure. Both examples suggest that the "annual cycle" cannot be "removed" by simply using a normalization procedure. The climate is not as completely represented when modelled as stationary processes.*

RÉSUMÉ *On introduit le processus cyclostationnaire dans l'analyse climatique et entreprend une étude systématique du spectre cyclique des fluctuations de la température de surface. Cette technique est une adaptation de la théorie de la cyclostationnarité dans le traitement des signaux. On en démontre l'utilité en construisant un modèle climatique cyclostationnaire stochastique très simple. Les résultats montrent que le cycle saisonnier module fortement les amplitudes de la covariance et du spectre. On a aussi appliqué la technique aux fluctuations de la température de surface dans un passage saisonnier de 15 ans du modèle CCM2, R15 (Community Climate Model) du NCAR en utilisant une surface moyenne symétriquement zonée comme couche limite basse. Les résultats indiquent que les oscilla-*

ATMOSPHERE-OCEAN 34 (4) 1996, 627–646 0705-5900/96/0000-0627$01.25/0

tions intrasaisonnières localisées selon le temps de l'année sont encore présentes après la normalisation des champs de température de surface à l'aide de procédures ordinaires. Les deux exemples indiquent que le «cycle annuel» ne peut etre «retranché» par une simple procédure de normalisation. Le climat n'est pas représenté aussi complètement lorsqu'il est modélisé par des processus stationnaires.

1 Introduction

In recent years interest has grown in the use of nonstationary random processes for modelling physical phenomena. This is due to the fact that many physical phenomena display nonstationary behaviour. Generally these phenomena have been modelled as stationary processes because the supporting theory is well developed. However, stationarity is a mathematical idealization which in some cases may not be a valid approximation. If these phenomena are to be better understood, they must be modelled as nonstationary processes.

In this paper we will deal with cyclostationary processes – a class of *nonstationary* processes whose joint variance and higher moments are periodical in time. Such processes commonly occur in a climate system due to periodic or quasi-periodic deterministic forcing (e.g., diurnal cycle, seasonal cycle, Milankovitch cycles, etc.). Recently, considerable attention has been given to applying cyclostationary techniques to the study of climatological time series (Bloomfield et al., 1994; Huang and North, 1996). Several prediction techniques for cyclostationary climate systems have also been developed and applied to the problem of predicting El Niño–Southern Oscillation (ENSO) events (Hasselmann and Barnett, 1981; Zwiers and von Storch, 1990).

Cyclostationary processes have also been called periodically correlated processes (Hurd, 1974), periodically nonstationary processes (Markelov, 1966; Ogura, 1971), and processes with periodic structure (Jones, 1964; Jones and Brelsford, 1967). Bennett (1958) was the first to introduce the term "cyclostationary processes" to denote the class of processes in his treatment of pulse sequences used in digital data transmission. The first mathematical treatment of these processes was by Gladyshev (1961) although Bennett (1958) discovered their characterizing property in the context of theoretic communication theory.

In order to give cyclostationary processes a precise meaning one must first establish some methods of characterizing the structures of these processes, such as spectral estimation, empirical orthogonal representation, etc. Gardner (1986, 1988, 1994) developed a number of techniques for estimating cyclic covariance and cyclic spectral densities for cyclostationary processes. These techniques have been applied in many studies (Gardner 1994), such as periodic-system identification, detection and extraction of modulated signals from corrupted data, etc. The present paper attempts to employ cyclic spectral analysis to a stochastic climate model, and to

the study of the seasonal variation of atmospheric temperature fluctuations at the earth's surface in a GCM simulation.

This study is partly motivated by the fact that climate fluctuations over a broad frequency range strongly depend on the time of year. For example, Lau and Lau (1986) noted that although the equatorial intraseasonal oscillations are present throughout the year, there exists a strong modulation of these modes by the seasonal cycle. Madden (1986) and Gutzler and Madden (1993) found these oscillations to be strongest during winter and weakest during summer. Recent studies have proposed that the irregularities of the interannual fluctuations, ENSO, can be viewed as a low-order chaotic process driven by the seasonal cycle (Jin et al., 1994; Tziperman et al., 1994).

Section 2 gives the background and basic concepts of the techniques of cyclic spectral analysis used in this study. The readers who have already had such background may skip this section and go directly to Section 3, in which the cyclostationary stochastic climate model and their cyclic spectra are described. Section 4 applies the cyclic spectral analysis to the seasonal variation of surface temperature fluctuations in a specific GCM simulation. In Section 5, we present the conclusions and discussions.

2 Cyclic Spectral Analysis

In this section we first briefly review some definitions and basic properties of cyclostationary processes and introduce the cyclic spectrum which will be used in our analysis. A comprehensive treatment of cyclostationarity in time series can be found in Gardner (1994) and references therein.

a *Definitions for a Cyclostationary Process*

The process $T(t)$ is stationary, if and only if the moments, such as the ensemble mean $M(t)$ and the covariance $C(t, t+\tau)$, are independent of time. If the mean $M(t)$ and covariance $C(t, t+\tau)$ exhibit periodicity d in time t, the process $T(t)$ is defined as a second order (wide sense) cyclostationary process with period d (Bennett, 1958; Gardner and Franks, 1975), i.e. for all t,

$$\begin{aligned} M(t+d) &= M(t) \\ C(t+d,\ t+d+\tau) &= C(t,\ t+\tau) \end{aligned} \tag{1}$$

If the mean $M(t)$ and covariance $C(t, t+\tau)$ exhibit the poly-periods $\{d\} = d_1, d_2, d_3, \cdots$, the process $T(t)$ is defined to be a poly-cyclostationary process with periods $\{d\}$. A process $T(t)$ is defined to be a higher-order cyclostationary process if its moments up to order k ($k > 2$) are periodic functions of time as in equation (1).

b *Cyclic Covariance*

The covariance given in (1) is periodic in t with period d for each value of τ. It is

assumed that the Fourier series representation for this periodic function converges, so that $C(t, t+\tau)$ can be expressed as

$$C(t,\ t+\tau) = \sum_{\alpha} C^{\alpha}(\tau) e^{i2\pi\alpha(t+\tau/2)}, \qquad \alpha = 0,\ \pm 1/d,\ \pm 2/d, \ldots \pm\infty \tag{2}$$

where $\{C^{\alpha}(\tau)\}$ are the Fourier coefficients,

$$C^{\alpha}(\tau) = \frac{1}{d} \int_{-d/2}^{d/2} C(t,\ t+\tau) e^{-i2\pi\alpha(t+\tau/2)} dt, \qquad \alpha = 0,\ \pm 1/d,\ \pm 2/d, \ldots \pm\infty \tag{3}$$

and α ranges over all integer multiples of the fundamental frequency $1/d$. The wave $\exp[i2\pi\alpha(t+\tau/2)]$ in the Fourier series introduced here contains a time shift $\tau/2$ so that the function $C(t+\tau/2, t-\tau/2)$ can be expanded in a Fourier series with the unshifted wave $\exp(i2\pi\alpha t)$ (Gardner, 1986, 1988, 1994). $C^{\alpha}(\tau)$ is called a cyclic-covariance at frequency α; the index α is referred as the cycle frequency parameter. It follows directly from (2) that the periodicity in the covariance $C(t, t+\tau)$ is completely characterized by the set of cyclic covariances $\{C^{\alpha}(\tau)\}$ indexed by α.

The cyclic covariance can be characterized in a way that reveals the role that periodicity in covariance plays in the frequency domain. We can reexpress the cyclic covariance (3) as

$$C^{\alpha}(\tau) = \frac{1}{d} \int_{-d/2}^{d/2} \langle [T(t)e^{-i\pi\alpha t}][T(t+\tau)e^{i\pi\alpha(t+\tau)}]^* \rangle dt \tag{4}$$

where the angular bracket $\langle \cdot \rangle$ denotes the ensemble average. That is, $C^{\alpha}(\tau)$ is actually a time-average cross-covariance for the two frequency-shifted processes

$$\langle C_{UV} \rangle(\tau) = \frac{1}{d} \int_{-d/2}^{d/2} \langle U(t)V^*(t+\tau) \rangle dt = C^{\alpha}(\tau) \tag{5}$$

where

$$U(t) = T(t)e^{-i\pi\alpha t} \tag{6}$$

and

$$V(t) = T(t)e^{+i\pi\alpha t} \tag{7}$$

are the frequency-shifted versions of $T(t)$. This reveals that a process exhibits cyclostationarity in the wide sense only if there exists a correlation between some frequency-shifted versions of the process.

c *Cyclic Spectrum*

It is well known that, for a stationary process, the power spectral density is defined as the Fourier transform of the covariance

$$S(f) = \int_{-\infty}^{+\infty} C(\tau) e^{-i2\pi f\tau} d\tau. \tag{8}$$

Similarly, it can be shown (cf. Gardner, 1988) that the cyclic spectral density is also equal to the Fourier transform of the cyclic covariance,

$$S^{\alpha}(f) = \int_{-\infty}^{+\infty} C^{\alpha}(\tau) e^{-i2\pi f\tau} d\tau. \tag{9}$$

It follows from (9) and (5) that the cyclic spectral density is the Fourier transform of the time-averaged cross-covariance $\langle C_{UV}\rangle(\tau)$ and is therefore identical to the time-averaged cross-spectral density for $U(t)$ and $V(t)$ given in (6) and (7):

$$S^{\alpha}(f) = \langle S_{UV}\rangle(f) \tag{10}$$

This is to be expected since the time-averaged cross-spectral density $\langle S_{UV}\rangle(f)$ is known to be the cyclic spectral density for spectral components in $U(t)$ and $V(t)$ at frequency f. Identity (10) suggests an appropriate standardization for $S^{\alpha}(f)$:

$$\langle S_U\rangle(f) = \langle S_T\rangle(f + \alpha/2) \tag{11}$$

$$\langle S_V(f)\rangle = \langle S_T\rangle(f - \alpha/2). \tag{12}$$

After standardization, the covariance becomes a correlation coefficient:

$$\frac{\langle S_{UV}\rangle(f)}{[\langle S_U\rangle(f)\langle S_V\rangle(f)]^{1/2}} = \frac{S^{\alpha}(f)}{[\langle S_T\rangle(f + \alpha/2)\langle S_T\rangle(f - \alpha/2)]^{1/2}} = \rho^{\alpha}(f) \tag{13}$$

Since $|\rho^{\alpha}(f)|$ is confined to the interval $[0, 1]$, it is a convenient measure of the degree of local spectral redundancy that results from the spectral correlation. The function $\rho^{\alpha}(f)$ is called the *autocoherence* function for $T(t)$. It is then clear that a process exhibits cyclostationarity in the wide sense only if there exists a correlation between distinct frequency components of the process. Moreover, the separation between any two such frequencies, $(f + \alpha/2) - (f - \alpha/2) = \alpha$, must be a cycle frequency of the process, (i.e., $\alpha = 1/d$).

Analogous to the duality of time- and frequency-domains for stationary processes one can define the time varying (instantaneous) spectral density as

$$S(t, f) = \int_{-\infty}^{+\infty} C(t, t + \tau) e^{-i2\pi f\tau} d\tau. \tag{14}$$

$S(t,f)$ is the time varying spectral density which is similar to the ordinary spectral density function (Gardner, 1994). It follows from (2) and (9) that the time varying spectral density for a cyclostationary process is completely characterized by the cyclic spectral density

$$S(t,f) = \sum_{\alpha} S^{\alpha}(f) e^{i2\pi\alpha t} \tag{15}$$

We can conclude from the foregoing discussions that the difference between stationary and cyclostationary or poly-cyclostationary processes is that the latter exhibit spectral correlation. Furthermore, this spectral correlation is completely and conveniently characterized by the cyclic spectra $\{S^{\alpha}\}$ or equivalently by the cyclic covariance $\{C^{\alpha}\}$. It is clear that essentially all the fundamental results of the theory of cyclic spectral analysis are generalizations of results from the conventional theory for stationary processes, and the latter is included as the special case of the former for which the cycle frequency α is zero (Gardner, 1986).

As an example, consider the amplitude-modulated signal

$$T(t) = w(t)\cos(2\pi f_0 t) - \frac{1}{2} w(t) e^{i2\pi f_0 t} + \frac{1}{2} w(t) e^{-i2\pi f_0 t} \tag{16}$$

for which $w(t)$ is a zero-mean stationary process. Since the exponential factors shift the frequency of each spectral component of $w(t)$ by $\pm f_0$, then there is obviously spectral correlation for all pairs of frequency components separated by $\alpha = 2f_0$. In fact the cyclic spectral density can be shown as

$$S^{\alpha}(f) = \begin{cases} \frac{1}{4} S_w(f + f_0) + \frac{1}{4} S_w(f - f_0), & \alpha = 0, \\ \frac{1}{4} S_w(f), & \alpha = \pm 2f_0, \\ 0, & \text{otherwise}, \end{cases} \tag{17}$$

where it has been assumed that $S_w(f) = 0$ for $|f| > 0.5$ to avoid an aliasing effect in the principal domain.

It follows from (13) that the spectral correlation coefficient is given by

$$\rho^{\alpha}(f) = \frac{S_w(f)}{\{[S_w(f + 2f_0) + S_w(f)][S_w(f) + S_w(f - 2f_0)]\}^{1/2}} \quad \text{for } \alpha = \pm 2f_0 \tag{18}$$

Thus, the correlation between the spectral component of $T(t)$ at frequencies $f + \alpha/2$ and $f - \alpha/2$ is unity:

$$|\rho^{\alpha}(f)| = 1 \text{ for } |f| < f_0 \text{ and } \alpha = \pm 2f_0, \tag{19}$$

provided that $w(t)$ is bandlimited to $|f| \leqslant f_0$,

$$S_w(f) = 0 \quad \text{for } |f| \geqslant f_0 \tag{20}$$

This is not surprising since the two spectral components in $T(t)$ at frequencies $f \pm \alpha/2 = f \pm f_0$ are obtained from the single spectral component in $T(t)$ at frequency f simply by shifting and scaling.

d *Estimation of the Cyclic Spectrum*

The theory and implementation of cyclic spectrum estimation algorithms has been covered in a number of publications. The basic time and frequency smoothing method of the cyclic spectrum is proposed by Gardner (1986). By itself, the time smoothed cyclic periodogram is not computationally efficient for computing estimates of the cyclic spectrum over large regions of the bifrequency plane. However, modification of the time and frequency smoothed cyclic periodogram leads to several computationally efficient algorithms. In general, a fast Fourier transform (FFT) based on time smoothing algorithms is considered most attractive for computing estimates of the cyclic spectrum over the entire bifrequency plane. The frequency smoothing method of the cyclic spectrum is best for computing estimates of the cyclic spectrum along the lines of constant cycle frequency of moderate values. A detailed review of estimation of the cyclic spectrum can be found in Roberts et al. (1994), and references therein.

3 Cyclostationary Stochastic Climate Model

As an example, we will consider a cyclostationary stochastic climate model. Stochastic climate models have been used in a variety of applications in recent years (Hasselmann, 1976; North and Cahalan, 1982; North et al., 1992 and many others). In these studies it is assumed that the evolution of a climatological function such as global average surface temperature $T(t)$ is governed by a Langevin-type equation

$$\frac{dT(t)}{dt} + aT(t) = F(t) \tag{21}$$

where t is time, a is a constant, and $F(t)$ is a broad band noise function. However, the feedback coefficient a, in many cases, will be seasonally variable. Hence, we introduce here a cyclostationary stochastic model by including periodic modulation of the feedback coefficient. In this case, (21) can be rewritten as

$$\frac{dT(t)}{dt} + (a + b\cos(\omega_0 t + \phi))T(t) = F(t) \tag{22}$$

where a and b are constants, $\omega_0 = 2\pi f_0$, and $f_0 = 1/d$ is the fundamental frequency such as the annual cycle. This is, of course, a very simplified model which is only intended as a mathematical example. We assume that $F(t)$ is white noise which satisfies

$$\begin{aligned} \langle F(t) \rangle &= 0 \\ \langle F(t)F(t') \rangle &= \sigma_F^2 \delta(t - t') \end{aligned} \tag{23}$$

where the angular brackets mean the ensemble average and δ is the Dirac delta function. The solution $T(t)$ of the inhomogeneous linear stochastic differential equation (22) can be written formally as

$$T(t) = e^{-(at+b^*\sin(\omega_0 t+\phi))} \int_{-\infty}^{t} F(t')e^{(at'+b^*\sin(\omega_0 t'+\phi))}dt' \tag{24}$$

where

$$b^* = \frac{b}{\omega_0}. \tag{25}$$

We note that in terms of the modified Bessel function $I_n(x)$

$$e^{(b^*\sin(\omega_0 t+\phi))} = \sum_{n=-\infty}^{+\infty} i^n I_n(b^*)e^{\{-in(\omega_0 t+\phi)\}} \tag{26}$$

Therefore the covariance function can be represented by the series

$C(t, t+\tau) =$

$$\begin{cases} \sigma_F^2 e^{-a\tau} \displaystyle\sum_{m,n,k=-\infty}^{+\infty} B_{mnk}(b^*) \frac{e^{i\omega_0(m+n-k)t}e^{i\omega_0 n\tau}e^{i\phi(m+n-k)}}{(2a - ik\omega_0)}, & \tau \geqslant 0 \\ \sigma_F^2 e^{a\tau} \displaystyle\sum_{m,n,k=-\infty}^{+\infty} B_{mnk}(b^*) \frac{e^{i\omega_0(m+n-k)t}e^{i\omega_0(n-k)\tau}e^{i\phi(m+n-k)}}{(2a - ik\omega_0)}, & \tau \leqslant 0 \end{cases} \tag{27}$$

where

$$B_{mnk}(b^*) = (i)^{m+n+k} I_m(b^*)I_n(b^*)I_k(2b^*). \tag{28}$$

Inserting the expression (27) into (3) we have the cyclic covariance

$C^\alpha(\tau) =$

$$\begin{cases} \sigma_F^2 e^{-a\tau} \displaystyle\sum_{m,n,k=-\infty}^{+\infty} B_{mnk}(b^*) \frac{e^{i\omega_0 n\tau}e^{-i\pi\alpha\tau}e^{i\phi(m+n-k)}\delta((m+n-k)f_0 - \alpha)}{(2a - ik\omega_0)}, & \tau \geqslant 0 \\ \sigma_F^2 e^{a\tau} \displaystyle\sum_{m,n,k=-\infty}^{+\infty} B_{mnk}(b^*) \frac{e^{i\omega_0(n-k)\tau}e^{-i\pi\alpha\tau}e^{i\phi(m+n-k)}\delta((m+n-k)f_0 - \alpha)}{(2a - ik\omega_0)}, & \tau \leqslant 0. \end{cases} \tag{29}$$

Using (9) it follows that

$S^\alpha(f) =$

$$\sigma_F^2 \sum_{m,n,k=-\infty}^{+\infty} B_{mnk}(b^*) \frac{e^{i\phi(m+n-k)}\delta((m+n-k)f_0 - \alpha)}{(a - i\omega_0 n + i\pi\alpha + i2\pi f)(a + i\omega_0(n-k) - i\pi\alpha - i2\pi f)}. \tag{30}$$

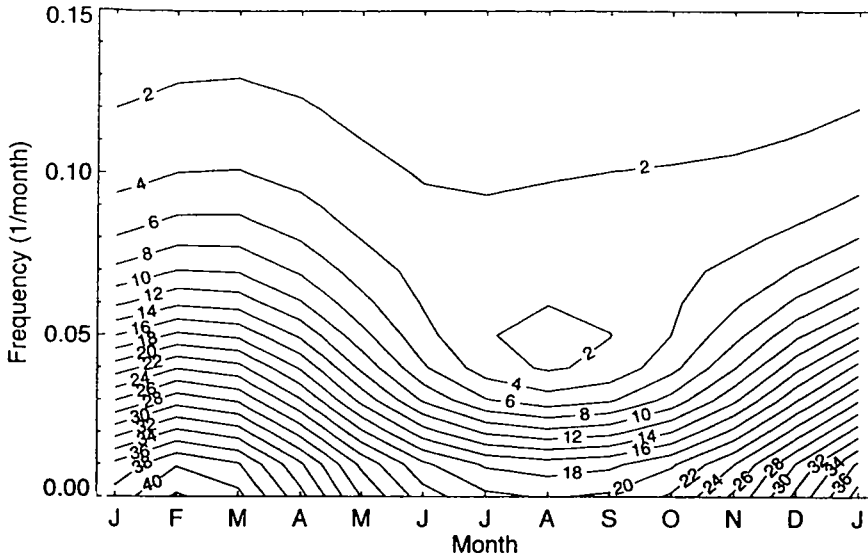

Fig. 1 Seasonal variation of spectra of the cyclostationary stochastic climate model.

As a numerical example for illustration, we have chosen: $a = 0.2$ month^{-1}, $b = 0.18$ month^{-1}, $f_0 = 1/d$, $d = 12$ month, corresponding to the annual cycle, $\phi = 72.5°$ and $\sigma_F^2 = 1.0$. Figure 1 shows the seasonal variation of the spectra $S(t,f)$ of this model with this set of values. The spectra decrease with increasing frequency in all months, which can be modelled to a good approximation as a first-order Markov process or "red noise". The spectra also exhibit a strong annual cycle with the maximum occuring in February and the minimum in August. Figure 2 shows the cyclic spectral density for $\alpha = 0$; $\alpha = 1/d$ and $\alpha = 2/d$ where α is the cycle frequency. The real part of cyclic spectral densities at $\alpha = 0$ (Fig. 2a) is a typical red spectrum. It is actually the average spectrum over the 12 months and is much stronger than the other components. But the annual component is also very clear while the semi-annual component becomes very small. According to Eq. (15), cyclic spectral densities are the Fourier coefficients of time varying spectra. The real and imaginary parts of the cyclic spectrum give the information about the amplitude and phase of each component. The seasonal variations of the spectra are characterized by the cyclic spectra $\{S^\alpha\}$. In this case, the first two components are the dominant ones. This result implies that the "annual cycle" cannot be "removed" by simply using the usual normalization procedure. To confirm this, we will apply the cyclic spectra analysis to the seasonal variation of surface temperature fluctuation in a GCM simulation in the next section.

4 Surface Fluctuation in a GCM Simulation

Observational studies indicate that the intraseasonal oscillations are particularly strong in and around the winter season (Knutson and Weickmann, 1987; Ghil and

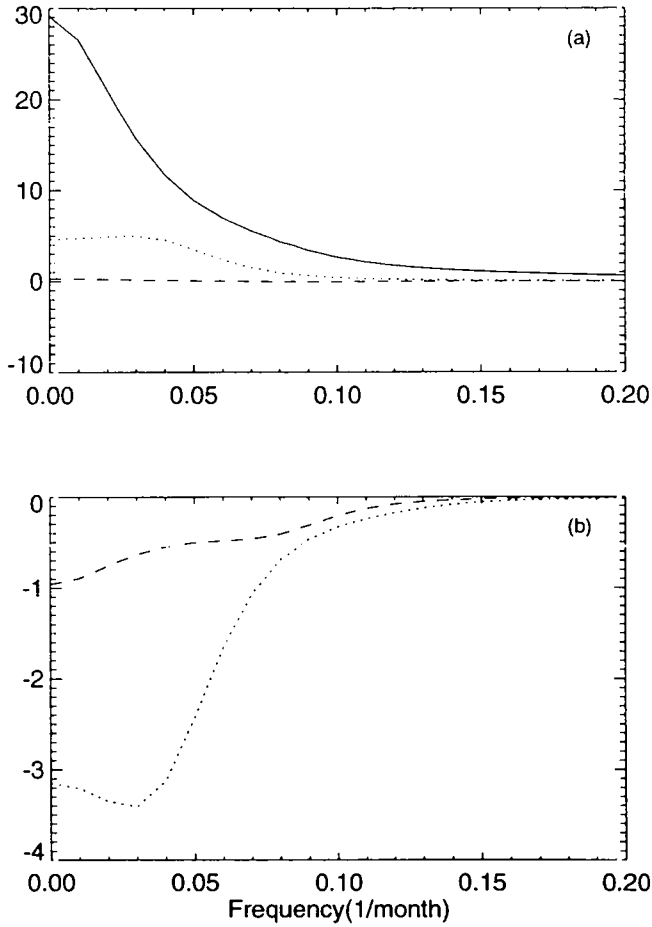

Fig. 2 Cyclic spectra of the cyclostationary stochastic climate model: (a) real part of cyclic spectral density; (b) imaginary part of cyclic spectral density. Solid line for $\alpha = 0$, short dashed line for $\alpha = 1/d$ and long dashed line for $\alpha = 2/d$, $d = 12$ month.

Mo, 1991; Dickey et al., 1991; Kimoto et al., 1991). Madden (1986) found that both the intensity and phase speed of intraseasonal oscillations exhibit seasonal variation with the strongest oscillations occuring during winter and the weakest during summer. Gutzler and Madden (1993) showed that the intraseasonal variability in the global momentum is largest in late winter and smallest in the fall season. However, these analyses are based on the assumption of stationarity. In this section we will use cyclic spectral analysis to show that intraseasonal oscillations are present in the simulated surface fields.

We have conducted a 15-year run of a seasonal climate model and will use the

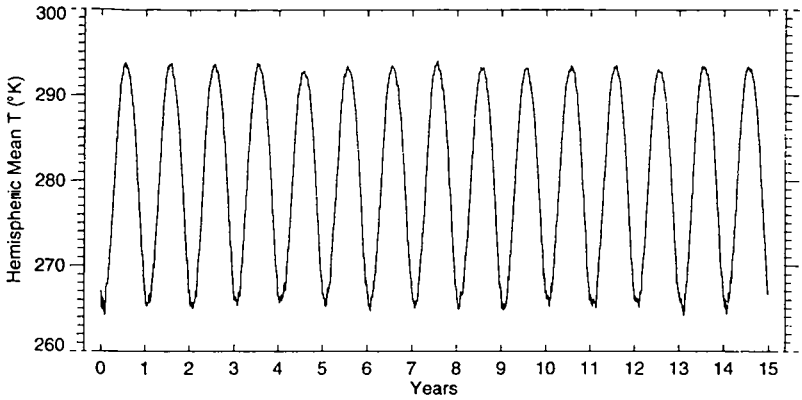

Fig. 3 Hemispherically-averaged daily surface temperature for the 15 years of simulation.

output as a further example of our procedures. We used the Community Climate Model version 2 (CCM2) developed at NCAR; the model uses the spectral method truncated at R15 with 18 vertical levels and is described in detail by Hack et al. (1993). To completely remove the asymmetric and external forcings, we idealized the boundary conditions. The idealized planet has no ocean, no topography, no snow cover and global uniform surface parameters (such as albedo, soil wetness factor). The simulations of this model planet at perpetual equinox with CCM0 and CCM2 have been discussed in some detail in North et al. (1992), North et al. (1993) and Yi et al. (1994). In this seasonal experiment, the declination angle will vary from $-11.75°$ to $11.75°$ over one year, so that the solar heating passes through annual cycles. The weaker seasonal forcing is used to prevent an excessively strong annual cycle on the all-land planet. No interannual variability will be introduced to the external forcing. We have also conducted a 15-year simulation without seasonal solar forcing. This simulation is referred to as the perpetual run.

Figure 3 presents the 15-year daily Northern Hemisphere averaged surface temperature. The time series shows 15 annual cycles with the minima in Dec–Jan–Feb (DJF) and maxima in June–July–Aug (JJA). The seasonal variability is much stronger than the interannual variability. Figure 4(a) shows the climatic and zonal mean of surface temperature. The climatic mean is the average of the data over 15 years for each day of the year. Comparing the variation in one hemisphere with that in the other hemisphere after shifting its phase by a half-year, we find that it is symmetrical with respect to the equator. In the equatorial region, the seasonal variations are very small because the solar irradiation does not change substantially throughout the year. In middle and high latitudes, a variation with a period of one year is dominant. To understand the contribution of a 30–50 day frequency component to the variance of surface temperature, we calculate the zonally averaged standard deviation of the unfiltered and 30–50 day band-pass filtered surface temperature. Time-filtering is accomplished by the use of a recursive digital filter

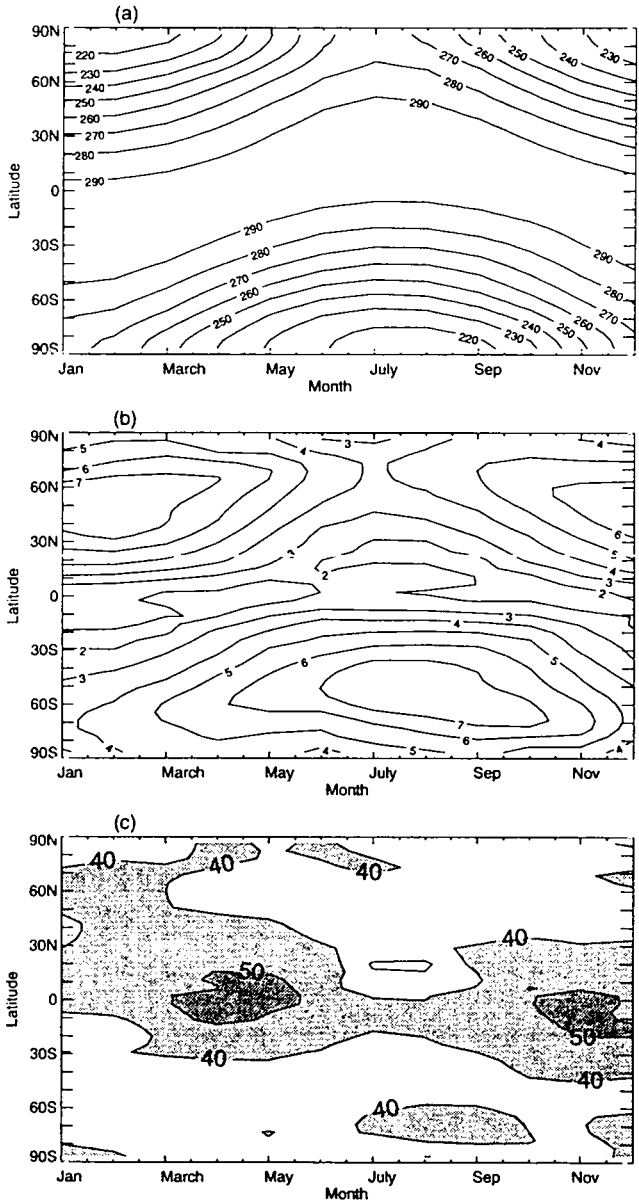

Fig. 4 The seasonal variation of simulation climate: (a) zonal mean surface temperature; (b) zonally-averaged standard deviation of the unfiltered surface temperature; (c) The ratio of the 30–50 day band-pass filtered standard deviation to the unfiltered standard deviation of surface temperature. Dark shade: $\geqslant$ 50%; middle shade: $\geqslant$ 40%; light shade: $\geqslant$ 30%.

(Murakami, 1979). The frequency response of a 30–50 day bandpass filter is designed in such a way that the amplitudes at 30- and 50-day periods are halved, while it is almost unchanged at a period of 40 days. Figure 4(b) shows the seasonal variation of the zonally-averaged standard deviation of the unfiltered surface temperature. As expected, the variability exhibits a strong seasonal cycle and is larger in the winter hemisphere especially over middle and high latitudes. Figure 4(c) shows the ratio of the 30–50 day band-pass filtered standard deviation to the unfiltered standard deviation. About 40–50% of the unfiltered standard deviation can be explained by 30–50 day low-frequency variability in the tropics and extratropics. The maxima are located at the equator during March and April, and in November. The 30–50 day low-frequency fluctuations account for a sizable fraction of the total variability, and it appears to be a global-scale phenomenon.

In the following we will represent the surface temperature fields as spherical harmonic coefficients with rhomboidal truncation $J = 15$

$$T(\mathbf{r}, t) = \sum_{m=-J}^{+J} \sum_{n=|m|}^{|m|+J} T_n^m(t) Y_n^m(\mathbf{r}) \tag{31}$$

where $Y_n^m(\mathbf{r})$ is the spherical harmonic function with degree n and zonal wavenumber m. The statistics were carried out on the spectral coefficients $T_n^m(t)$. We found that the modes with wavenumber $m = 1$ and $(n - m) = 0 - 2$ have the highest variance.

To examine the effect of the seasonal forcing on the intraseasonal oscillation, the usual practice is to remove the annual cycle from the data prior to the spectral analysis by using the normalization

$$T_n^{m\prime} = \frac{T_n^m - \overline{T_n^m}}{\sigma(T_n^m)} \tag{32}$$

Here $\overline{T_n^m}$ is the 15-year climatic mean of daily data and $\sigma(T_n^m)$ is the standard deviation which is calculated as

$$\sigma(T_n^m) = \sqrt{\sum_{k=1}^{K} (T_{nk}^m - \overline{T_n^m})(T_{nk}^m - \overline{T_n^m})^* / (K - 1)} \tag{33}$$

where k is an index indicating the number of the year, K is the total number of years of data ($K = 15$). It is often assumed that the oscillations are superimposed on the annual cycle and the annual cycle can be "removed" by simply using the normalization procedure. In other words, the normalized data is considered to be stationary. If this were the case, the spectra of oscillations could not be localized according to time of year.

We will apply the cyclic spectral analysis techniques to identify any remaining seasonal variation of oscillation in $T_n^{m\prime}$. The algorithm used for computing estimates

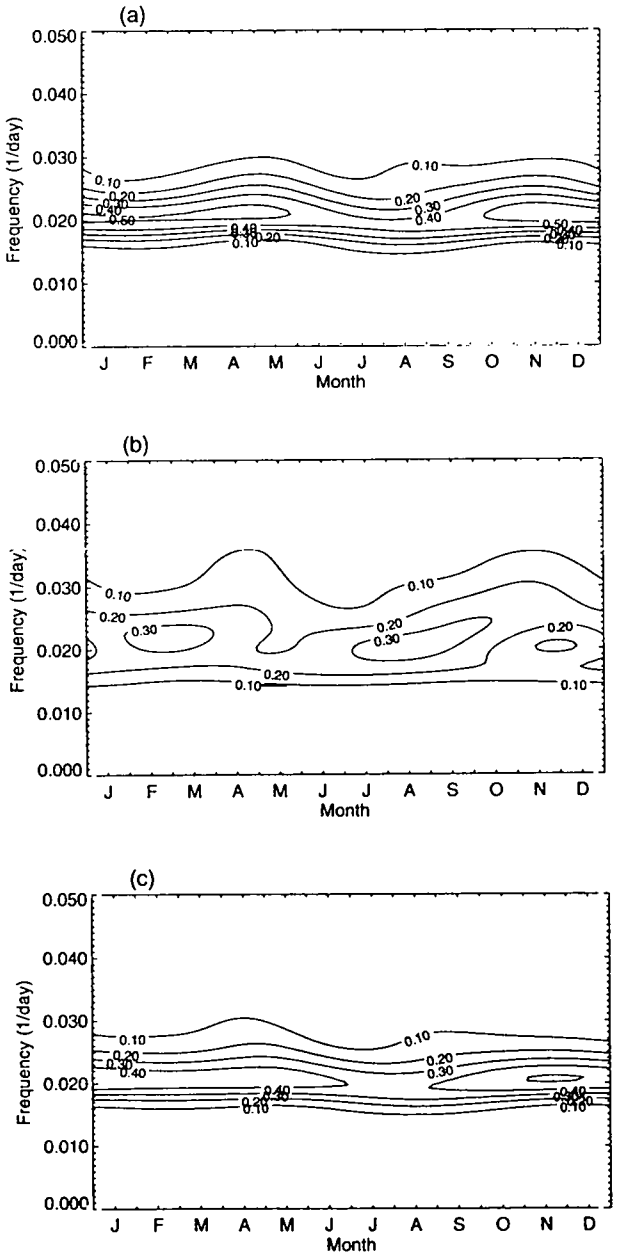

Fig. 5 The seasonal variation of spectra for normalized spherical harmonic coefficients of surface temperature ($T_n^{m'}$) for: (a) $m = 1$, $n = 1$; (b) $m = 1$, $n = 2$; (c) $m = 1$, $n = 3$.

of cyclic spectra is the FFT based on a time smoothing algorithm. For details of the algorithm, the reader is referred to Roberts et al. (1994).

Figure 5 shows the seasonal variation of spectra for the three modes with highest variance. There are obvious oscillations at 40–50 day periods with significant seasonal variability. Figure 5 indicates that for both modes $m = 1$, $n = 1$ and $m = 1$, $n = 3$ the variance in the 50-day band has a relative maximum from October through May, while that for mode $m = 1$, $n = 2$ has two relative maxima in late winter–early spring and in late summer. Figure 6 shows another three modes with: (a) $m = 2$, $n = 4$; (b) $m = 3$, $n = 5$; (c) $m = 4$, $n = 6$. Figure 7 shows the seasonal variation of spectra for mode $m = 1$, $n = 1$ for: (a) surface sensible heat flux; (b) surface latent heat flux; (c) net upward longwave flux at the top of the atmosphere. All three fields show the ubiquitous feature of intraseasonal variability. Intraseasonal variance in either sensible heat flux or surface latent heat flux is strong in winter and weak in summer. These results indicate that the presence of intraseasonal oscillations in surface fields is also localized according to time of year. These season-frequency localizations are impossible to obtain by conventional spectral analysis.

As a comparison with conventional spectral analysis, Fig. 8 shows the normalized space-time power spectral density of surface temperature for wavenumber one at four latitudes. The solid line represents the spectral density of the perpetual run, while the dashed line represents the seasonal run. A conspicuous spectral peak with a period around 40–50 days occurs in both spectral densities. These spectral peaks represent waves which propagate eastward and take about 40–50 days to encircle the globe. However, the peak of the seasonal run is shifted from 40 days to 50 days. Another interesting feature to note is that the peak of the seasonal run is stronger than the perpetual run, especially in middle and high latitudes. One may therefore infer that the seasonal forcing not only modulates but also enhances the intraseasonal oscillation. However, as we mentioned above, this feature is season-dependent. The Fourier transform of conventional spectral analysis can identify the intraseasonal oscillations, but it gives no information regarding their seasonal dependence since the spectra are averaged over the entire data record. In addition, the "annual cycle" cannot be "removed" completely by simply using the normalization. The climate is not as completely represented when modelled as stationary processes.

5 Conclusions and Discussions

In this paper we provide the basic framework and some examples of the application of cyclic spectral analysis to climate studies. A process is said to exhibit cyclostationarity in the wide sense if its covariance $C(t, t+\tau)$ is periodic in t. The Fourier coefficient $C^{\alpha}(\tau)$ of the covariance function is called the cyclic covariance with cycle frequency α. The Fourier transform $S^{\alpha}(f)$ of the cyclic covariance is called the cyclic spectrum. The difference between stationary and cyclostationary

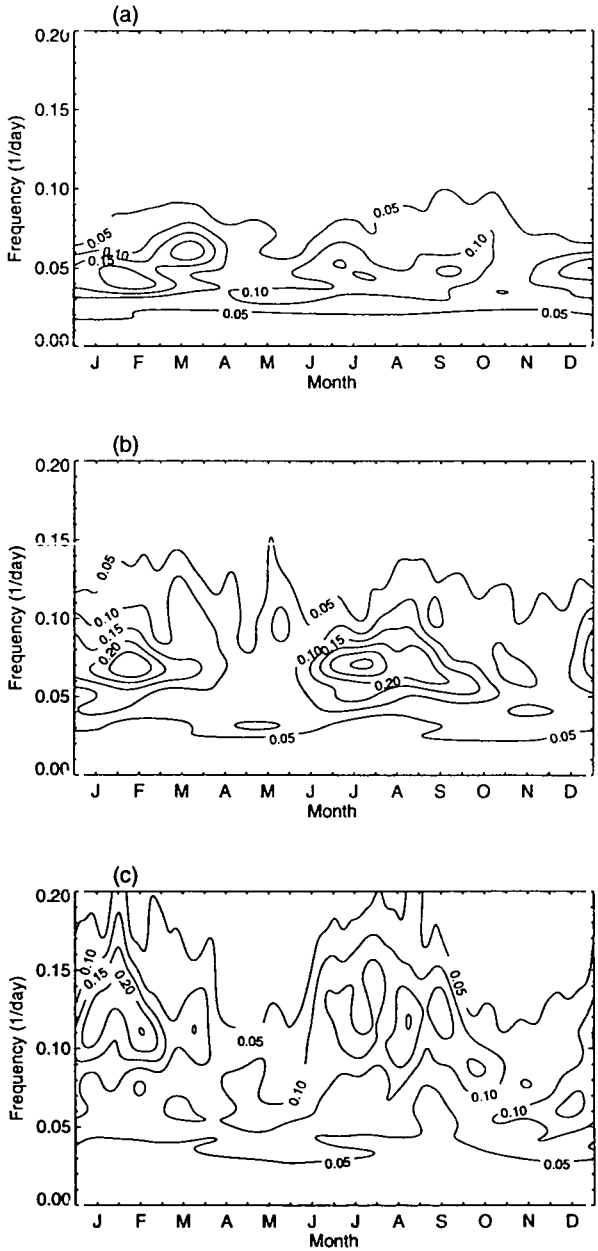

Fig. 6 As in Fig. 5 but for: (a) $m = 2$, $n = 4$; (b) $m = 3$, $n = 5$; (c) $m = 4$, $n = 6$.

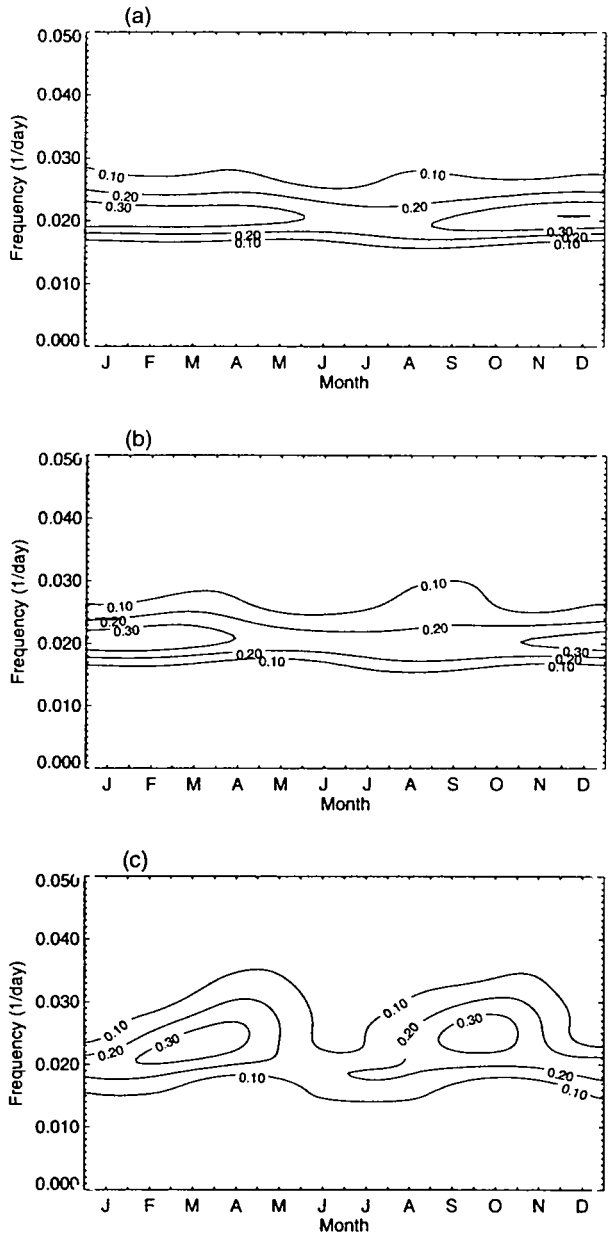

Fig. 7 As in Fig. 5 but for (a) surface sensible heat flux; (b) surface latent heat flux; (c) net upward long wave flux at the top of atmosphere.

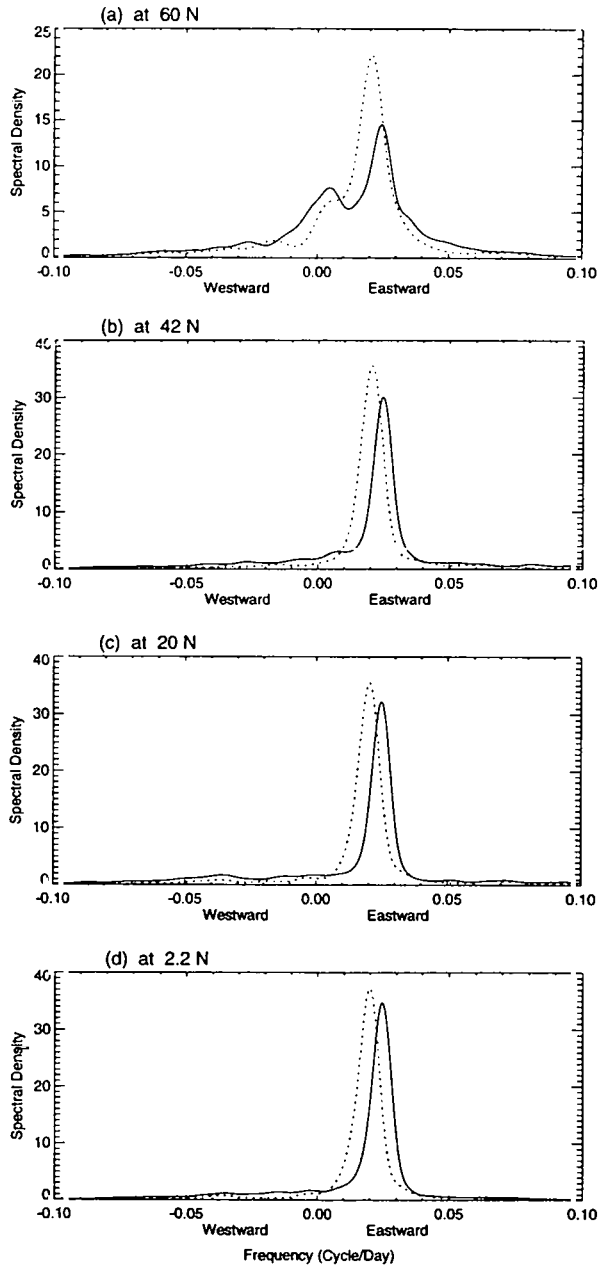

Fig. 8 The standardized space-time power spectral density of the surface temperature for wavenumber one at (a) 60°N; (b) 40°N; (c) 20°N; (d) 2.2°N. The solid line represents the spectral density of the perpetual run, while the dashed line represents the seasonal run.

processes is that the latter exhibit spectral correlation between spectral components at frequencies separated by 2α.

To demonstrate the usefulness of this technique, a very simple cyclostationary stochastic climate model is constructed. This simple model describes the global average surface temperature. Our results show that the seasonal cycle strongly modulates the amplitude of the covariance and spectrum. The surface temperature fluctuations on a zonally symmetric all-land planet with seasonal solar forcing have also been studied. The results indicate that the presence of intraseasonal oscillations in surface fields is dependent on the season, although the surface fields have been normalized before we compute the cyclic spectra. The strength of the intraseasonal oscillations is strongest during winter and weakest during summer. Both examples suggest that the "annual cycle" cannot be "removed" by simply using the usual normalization procedure. The climate is not as completely represented when modelled as a stationary process. It should become clear from the foregoing examples that our characterization of the variations using cyclic spectral analysis contains more information than the conventional spectral analysis.

The cyclic spectral analysis has many applications. Another example is to detect and classify multiple fluctuations buried in noise. This would be impossible to accomplish using only conventional spectral analysis (cyclic spectra at $\alpha = 0$). This application will be the subject of a subsequent publication.

Acknowledgments

We thank Y.-H. Yi for her kind assistance with some data processing. We would also like to thank Dr. Peter Bartello and the anonymous reviewers for their helpful comments on the manuscript. This research was supported by research grants from the Canadian Natural Science and Engineering Research Council, and the Atmospheric Environment Service of Canada.

References

BENNETT, W.R. 1958. Statistics of regenerative digital transmission. *Bell. Syst. Tech. J.* **37**: 1501–1542.

BLOOMFIELD, P., H.L. HURD and R.B. LUND. 1994. Periodic correlation in stratospheric ozone data. *J. Time Series Anal.* **15**: 127–150.

DICKEY, J.O., M. GHIL and S.L. MARCUS. 1991. Extratropical aspects of the 40–50 day oscillation in length-of-day and atmospheric angular momentum. *J. Geophys. Res.* **96(D12)**: 22643–22658.

GARDNER, W.A. 1986. The spectral correlation theory of cyclostationary time-series. *Signal Processing*, **11**: 13–36.

———. 1988. *Statistical Spectral Analysis: A Nonprobabilistic Theory*, *Prentice Hall*, pp. 301–359.

———. 1994. An introduction to cyclostationary signals. In: *Cyclostationarity in communications and signal processing*. W.A. Gardner, (Ed.) IEEE Press, pp. 1–90.

——— and L.E. FRANKS. 1975. Characterization of cyclostationary random processes. *IEEE Trans. Inform. Theory*, **21**: 4–14.

GHIL, M. and K.C. MO. 1991. Intraseasonal oscillation in the global atmosphere. Part I: Northern Hemisphere and tropics. *J. Atmos. Sci.* **48**: 752–779.

GLADYŠEV, E.G. 1961. Periodically correlated random sequences, *Soviet Math.* **2**: 385–388.

GUTZLER, D.S. and R.A. MADDEN. 1993. Seasonal variations of the 40 ~ 50-day oscillation in atmospheric angular momentum. *J. Atmos. Sci.* **50**: 850–860.

HACK, J.J.; B.A. BOVILLE, B.P. BRIEGLEB, J.T. KIEHL, P.J. RASCH and D.L. WILLIAMSON. 1993. Description of the NCAR Community Climate Climate Model (CCM2). NCAR Tech. Note, NCAR/TN-382+STR, NCAR, Boulder, Colorado, 108 pp.

HASSELMANN, K. 1976. Stochastic climate model. *Tellus*, **28**: 473–485.

——— and T.P. BARNETT. 1981. Techniques of linear prediction for a system with periodic statistics. *J. Atmos. Sci.* **38**: 2275–2283.

HUANG, J.-P. and NORTH, G.R. 1996. Cyclic spectral analysis of fluctuations in a GCM simulation. *J. Atmos. Sci.* **53**: 370–379.

HURD, H.L. 1974. Periodically correlated processes with discontinuous correlation functions. *Theory Prob. Appls.* **19**: 804–807.

JIN, F.-F.; J.D. NEELIN and M. GHIL. 1994. El Niño on the devil's staircase: annual subharmonic steps to chaos. *Science*, **264**: 70–72.

JONES, R.H. 1964. Spectral analysis and linear prediction of meteorological time series, *J. Appl. Meteorol.* **3**: 45–52.

——— and W.M. BRELSFORD. 1967. Time series with periodic structure, *Biometrika*, **54**: 403–407.

KIMOTO, M.; M. GHIL and K.-C. MO. 1991. Spatial structure of the 40 day oscillation in the Northern Hemisphere extratropics. Proc. 8th Conf. Atmos. Ocean. Waves and Stability, Amer. Meteorol. Soc., Boston, pp. 115–116.

KNUTSON, T.R. and K.M. WEICKMANN. 1987. 30–60 day atmospheric oscillations: composite life cycles of convection and circulation anomalies. *Mon. Weather Rev.* **115**: 1407–1436.

LAU, N.-C. and K.-M. LAU. 1986. The structure and propagation of intraseasonal oscillations appearing in a GFDL general circulation model. *J. Atmos. Sci.* **43**: 2023–2047.

MADDEN, R.A. 1986. Seasonal variation of the 40 ~ 50 day oscillation in the tropics. *J. Atmos. Sci.* **43**: 3138–3158.

MARKELOV, V.A. 1966. Axis crossings and relative time of existence of a periodically nonstationary random process, *Sov. Radiophys.* **9**: 440–443.

MURAKAMI, M. 1979. Large-scale aspects of deep convective activity over GATE area. *Mon. Weather Rev.* **107**: 994–1013.

NORTH, G.R. and R.F. CAHALAN. 1982. Predictability in a Solvable Stochastic Climate Model. *J. Atmos. Sci.* **38**: 504–513.

———; K.-Y. YIP, R. LEUNG and R. CHERVIN. 1992. Forced and free variations of the surface temperature field in a GCM. *J. Clim.* **5**: 227–239.

———; R.E. BELL and J.W. HARDIN. 1993. Fluctuation dissipation in a general circulation model. *Clim. Dyn.* **8**: 259–264.

OGURA, H. 1971. Spectral representation of periodic nonstationary random processes. *IEEE Trans. Inform. Theory*, **17**: 143–149.

ROBERTS, R.S.; W.A. BROWN and H.H. LOOMIS, JR. 1994. A review of digital spectral correlation analysis: theory and implementation. In: *Cyclostationarity in communications and signal processing.* W.A. Gardner, (Ed.) IEEE Press, pp. 455–479.

TZIPERMAN, E.; L. STONE, M.A. CANE and H. JAROH. 1994. El Niño chaos: Overlapping of resonances between the seasonal cycle and the Pacific ocean-atmosphere oscillator. *Science*, **264**: 72–74.

YI, Y.-H.; J.-P. HUANG, G.R. NORTH and K.P. BOWMAN. 1994. Circulation Statistics For CCM2 Terra Blanda. CSRP Tech. Report No. 2, Texas A&M University, 88 pp.

ZWIERS, F. and H. VON STORCH. 1990. Regime-dependent autoregressive time series modeling of the southern oscillation. *J. Clim.* **3**: 1347–1368.